IJARSCT
ISSN (Online) 2581-9429
International Journal of Advanced Research in Science, Communication and Technology (IJARSCT)
Volume 2, Issue 1, June 2022
Impact Factor: 6.252

Crop Leaf Disease Detection and Classification Using Deep Learning Algorithm

Dr. G. Nanthakumar (M.E., Ph.D,)[1], Athileshwaran T[2], Abinash. P[3]
Professor, Department of Science and Computer Engineering[1]
Final Year Students, Department of Science and Computer Engineering[2,3]
Anjalai Ammal Mahalingam Engineering College, Kovilvenni, Tiruvarur, Tamil Nadu, India
nanthashriram@gmail.com, athileshwarant@gmail.com, abinash722000@gmail.com

Abstract: *Plant disease identification is vital for agriculture because it is essential for enhancing crop yields. Visual plant disease analysis is a novel technique to handle this problem because to recent developments in image processing. There are, however, few works in this field, let alone comprehensive studies. We investigate the challenge of visual plant disease detection for plant disease diagnosis in this research. Plant disease photos, in comparison to other types of photographs, tend to have randomly dispersed lesions, varied symptoms, and complex backgrounds, making discriminative information difficult to capture. We created a new large-scale plant disease dataset containing 271 plant disease categories and 220,592 photos to aid plant disease recognition studies. We approach plant disease recognition using this dataset to emphasise sick portions by reweighting both visual regions and loss to determine the discriminative level of each patch, we first compute the weights of all the divided patches from each image based on the cluster distribution of these patches. Then, during weakly-supervised training, we assign weight to each loss for each patch-label pair to enable discriminative disease component learning. Finally, we use the LSTM network to encode the weighed patch feature sequence into a comprehensive feature representation, extracting patch features from the network trained with loss reweighting. Extensive tests on this and another publicly available datasets show that the proposed strategy is superior. We anticipate that our study will advance the plant disease recognition agenda in the image processing community.*

Keywords: Convolutional neural network (CNN), Active Contour Method, Deep learning.

I. INTRODUCTION

Plant diseases pose a serious danger to global food security because they reduce agricultural productivity around the world. Plant diseases are responsible for 20 percent to 40 percent of all crop losses worldwide, according to figures. As a result, plant disease identification is crucial for preventing the spread of plant diseases and reducing agricultural economic losses. The majority of plant disease diagnosis approaches rely primarily on either a molecular assay or the observation of a plant protector. However, the former is time-consuming and prone to errors, while the latter is sophisticated and limited to centralised labs. The latter, on the other hand, is time consuming and prone to errors. Currently, image-based technologies are being widely used to understand visual material in a variety of interdisciplinary activities, such as medical imaging, food computing, and cellular image analysis. We believe that plant picture analysis and recognition can give a new technique for plant disease diagnosis, thanks to recent breakthroughs in machine learning, particularly deep learning. In the meantime, applications in visual plant disease diagnostics encourage the advancement of image processing technologies.

Aerial phenotyping and leaf fingerprinting are two examples of plant image analysis study and exploration in this sector. However, because these procedures rely largely on either pricey instruments or complicated chemical technology, they are difficult to mainstream. Some recent studies have used deep learning approaches to recognise plant diseases. However, the majority of them extract deep features from plant disease photos without taking task characteristics into account. Furthermore, these projects are limited to small datasets with fewer categories and plain graphic backgrounds.

1.1 Deep Learning

To build a deep learning model, you'll need to design numerous algorithms, combine them, and form a network of neurons. Deep learning is computationally expensive. Tensor flow, Py-Torch, Chainer, Keras, and other deep learning

IJARSCT
ISSN (Online) 2581-9429
International Journal of Advanced Research in Science, Communication and Technology (IJARSCT)
Volume 2, Issue 1, June 2022
Impact Factor: 6.252

platforms exist to enable deep learning models. In deep learning, we've attempted to duplicate the human brain network with an artificial neural network; in the deep learning model, the human neuron is referred to as a perceptron. We establish a neural network by connecting these perceptron units together; it comprises three sections:

- Hidden layers
- Input layer
- Output layer

Input nodes (dendrites in the human brain), an actuation function for making a small decision, and output nodes make up a perceptron (axon in the human brain). We'll look at how one perceptron works before putting them all together to make a deep learning model. The actuation function receives input data (number of input variables/features) that has been given some weight. The actuation function makes a choice and transmits a signal. The output of this perceptron will be sent into other neurons. Backpropagation error is determined at each neuron using a cost function/cross-entropy after the batch has been processed. As a result, input weights are redistributed, and the process repeats until cross-entropy meets the requirement. To create the Deep Learning model, the popular architectures are RNN, CNN, etc.

1.2 Convolutional Neural Network

A convolutional neural network (CNN) is a deep learning technique created primarily for image processing. In image recognition and processing, convoluted neural networks are used.

A CNN's neural networks are organised in the same way as the frontal lobe of the human brain, which is responsible for processing visual inputs. The convolutional neural network is made up of the following components:

A convolutional layer, a pooling layer, a fully connected input layer, a fully connected layer, and a fully connected output layer are all examples of completely connected layers. Convolution neural networks have been limited in their application for a long time due to scaling difficulties. For efficiency, these neural networks required a large amount of training data, and they were only suitable for low-resolution images. AlexNet, on the other hand, has reintroduced multi-layered neural networks and employed big data sets from the ImageNet data set since 2012, allowing complex convolutional neural networks to be created.

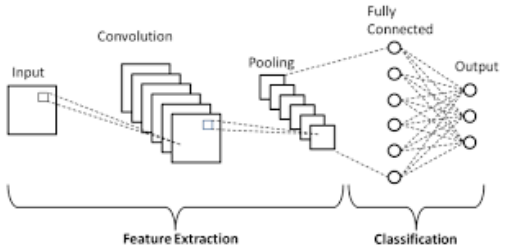

Fig. 1.2.a. Convolutional Neural Network process flow

1.3 Active Contour Method

Active contour is a segmentation approach that uses energy forces and restrictions to separate the pixels of interest from the remainder of the image for further processing and analysis. The term "active contour" refers to a model that is used in the segmentation process. Contours are lines that define the area of interest in a photograph. A contour is a grouping of points that has been interpolated. The interpolation procedure, which describes the curve in the image, might be linear, splines, or polynomial. In image processing, different models of active contours are used in the segmentation procedure. The most common use of active contours in image processing is to define a smooth shape in an image and create a closed contour for a region. Snake models, gradient vector flow snake models, balloon models, and geometric or geodesic contours are examples of active contour models.

II. LITRATURE REVIEW

Ghaiwat et al. give a review of the many classification strategies that can be used to classify plant leaf diseases. For the current test case, the k-nearest-neighbour method appears to be the most appropriate and straightforward of the class

IJARSCT
ISSN (Online) 2581-9429
International Journal of Advanced Research in Science, Communication and Technology (IJARSCT)
Volume 2, Issue 1, June 2022
Impact Factor: 6.252

prediction methods. It is difficult to establish ideal parameters in SVM if the training data is not linearly separable, which appears to be one of its shortcomings [1].

Mrunalini et al. [3] describe a method for classifying and identifying plant diseases. Machine learning-based recognition systems will be very valuable in the Indian economy because they save time, money, and effort. The colour co-occurrence method is used in this article for feature set extraction. Neural networks are used to automatically detect illnesses in leaves. The proposed method can considerably help with accurate leaf detection and appears to be a useful method in the event of steam and root infections, while requiring less computational work.

According to paper [4], the disease detection process consists of several processes, the four most important of which are as follows: A colour transformation structure is first created for the input RGB image, and then the green pixels are masked and deleted using a certain threshold value, followed by a segmentation procedure, and finally texture statistics are computed to obtain useable segments. Finally, the features retrieved to classify the disease are sent into a classifier. The suggested algorithm's resilience is demonstrated using experimental findings from roughly 500 plant leaves in a database.

Kulkarni et al. describe a method for detecting plant illnesses early and accurately utilising an artificial neural network (ANN) and other image processing techniques. Because the suggested method uses an ANN classifier for classification and a Gabor filter for feature extraction, it produces better results, with a recognition rate of up to 91%. An ANN-based classifier classifies distinct plant diseases and recognises them using a mix of textures, colours, and characteristics [5].

III. PROPOSED SYSTEM

Automatic leaf disease identification is an important research subject in agriculture because it can help monitor huge fields of crops. Extraction of high-level attributes such as colour, shape, and texture using image processing algorithms. Segment the tree leaves using the Graph Cut algorithm, based on the pixel intensity of the green component. To classify diseases and make fertiliser recommendations, use the convolutional neural network approach. The CNN is a very powerful approach that has been widely employed in a range of image categorization applications. It has sparked interest in a variety of fields, including image recognition, image analysis, object detection, and computer vision jobs. The CNN rapidly extracts information from photos, and its hierarchical structure enables it to deal with images in real time. Each convolution stage produces a new "convolved" image that includes features from the previous step. The advantages of this proposed system leads to segmentation that is automated, features that are relevant are extracted and several leaf diseases have been found. The accuracy rate is quite high.

IV. DATASET CONSTRUCTION

Building a large-scale, high-quality dataset is difficult due to the complexity, diversity, and variability of plant diseases. To begin, agricultural datasets should be annotated by a variety of experts from various sectors. Annotating illnesses on apple fruit trees and juglans, for example, necessitates different expertise, which is demand-driven and time-consuming. Second, time and location constrain the collection of plant disease photos.

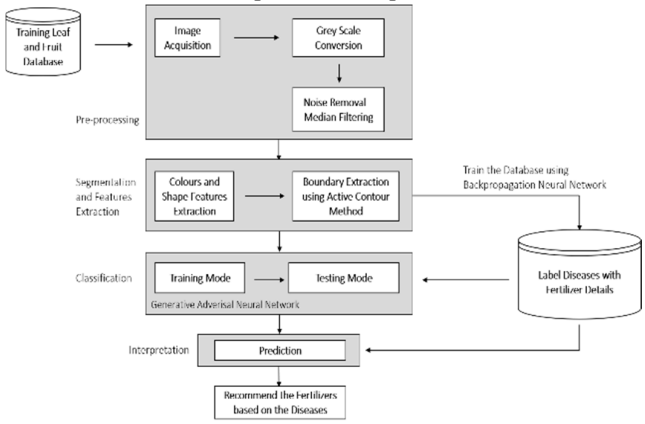

Fig. 3. System Architecture for leaf disease detection

IJARSCT
ISSN (Online) 2581-9429
International Journal of Advanced Research in Science, Communication and Technology (IJARSCT)
Volume 2, Issue 1, June 2022
Impact Factor: 6.252

The data building process is comprised of the three components below.

(1) Establishment of a taxonomic system. For the PDD271 dataset, we create a four-layer hierarchical taxonomic system. We invite a panel of agricultural specialists to examine the most prevalent types of plant illnesses that people encounter on a daily basis. Each disease is given an upper-level classification based on the plant that is afflicted. And, depending on the planting circumstances and plant morphology, each plant is assigned to an upper-level class. For example, the apple brown spot, ruins the apple, which belongs to the fruit tree. Finally, we build a structure of 1, 3, 43, and 271 nodes in the first, second, third, and fourth layers, respectively, with the dataset root, macro-classes, plant categories, and plant illnesses. The findings of the plant disease hierarchy visualisation are shown in Fig. 4.

(2) Dataset gathering.

We form ten teams in order to acquire a big number of illness images. Each team consists of eight agriculture university students and four professionals in related subjects. Each team collects thirty different diseases, each of which has over 500 different photos from various plants. Experts are in charge of ensuring the quality of illness photos and annotations. One usual strategy for obtaining photographs is to keep the distance between the camera and the plant between [20cm,30cm] to provide a similar visual scope. Every plant disease category has at least 500 photos, and each category has more than 200 plants. Furthermore, a single plant can be photographed from many perspectives.

(3) Dataset expansion and processing.

Following image collecting, each image is double-checked by three specialists to ensure label accuracy. Then, to keep the dataset clean, professionals delete blurry photos and other noisy images. We collect extra photographs for categories with fewer images to ensure that each category's image number is met. In order to create image processing technology in a certain domain, a dependable dataset is required. HiEve [38], for example, is critical for human-centric analyses, whereas ATRW [39] is critical for animal conservation. Similarly, the proposed dataset PDD271 encompasses a wide range of plant diseases. It will advance the plant disease recognition agenda and broaden the application of image processing technology to the agriculture sector.

Fig. 4. Taxonomy of the PDD271 dataset

V. MODULE DESCRIPTION

- Leaf image acquisition.
- Preprocessing.
- Leaf segmentation.
- Disease prediction.
- Recommendation of solution.

5.1 Leaf Image Acquisition

Leaves are photosynthesis-specialized structures that are placed on the tree to maximise their exposure to light while avoiding shadowing one another. We can upload the leaf photos from the datasets to this module.

IJARSCT
ISSN (Online) 2581-9429
International Journal of Advanced Research in Science, Communication and Technology (IJARSCT)
Volume 2, Issue 1, June 2022
Impact Factor: 6.252

This dataset is made up of shape and texture attributes taken from digital photographs of leaf specimens from a variety of plant species.

To distinguish the leaf section of the image from the backdrop, edge detection, filtering, and thresholding methods were used. When using the electronic planimeter to measure the leaf area, the relative error rate of the software's estimates was less than 7%, with the highest relative error rate when using the scanner and the lowest when using the digital camera. Regardless of the equipment utilised for image capture, Pearson's correlation coefficients were higher than 95%, showing that the programme was able to generate reliable estimations of leaf area.

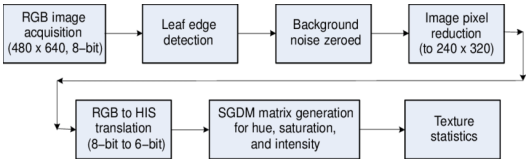

Fig. 5.1.a. Leaf Image Acquisition flowchart

5.2 Preprocessing

Steps that are required to do pre-processing are as follows:

Data Cleaning/Cleansing.

Data that has been deemed "dirty" must be cleaned. Data in the real world is frequently incomplete, noisy, and inconsistent.

Data Integration.

Data from several sources is combined.

Data Transformation.

Creating a data cube.

Data reduction.

Reducing the size of the data set's representation.

In our research, the RGB image is converted to grayscale in this module. Leaves are constantly green in colour, and the variety of changes in the environment causes the colour feature to be unreliable. As a result, the received leaf picture in RGB format will be transformed to grey scale before pre-processing in order to recognise distinct plants using their leaves. Then, using filtering techniques, remove the noise from the photos. The filter's purpose is to remove noise that has distorted the image. It employs a statistical technique. Filters are typically intended to have a specific frequency response.

5.3 Leaf Segmentation:

We can use the graph cut method with automatic descriptors in this module. Unconstrained borders applied to the intricate natural imagery we're working with would result in disappointing contours that tried to squeeze through every crevice and aw in the leaf's border. The method we propose is to use the polygonal model created in the first phase not only as an initial leaf contour, but also as a shape prior that will steer the evolution of the model toward the true leaf boundary.

5.4 Disease Prediction

Bacteria, fungus, viruses, and other insects all harm the leaves. Use a convolutional neural network technique to categorise the leaf picture as normal or impacted in this module. Leaf properties such as colour, shape, and texture are used to create vectors. Then, using conditions, layers can be built to categorise the pre-processed leaves. Also, by using a multiclass classifier, we can more accurately forecast illnesses in leaf photos.

5.5 Recommendation of Solution

This module will suggest a fertiliser for injured leaves based on their severity. Organic and inorganic fertilisers are both available. The fertilisers can be stored by the administrator based on disease classification and severity levels. Fertilizer measurements can be derived based on illness severity.

IJARSCT
ISSN (Online) 2581-9429
International Journal of Advanced Research in Science, Communication and Technology (IJARSCT)
Volume 2, Issue 1, June 2022
Impact Factor: 6.252

VI. EXPERIMENT

6.1 Experimental Setting

1) Dataset Split and Metric: The PDD271 contains 220,592 pictures divided into 271 disease classifications. A roughly 7: 2: 1 split is followed. There are 154,701 training, 44,002 validation, and 21,889 testing images in the PDD271. As the evaluation metric, the top-1 classification accuracy is used.

2) Hyperparameter Setting: All photos have been scaled to 224 224 pixels. Each image is broken down into four patches. With the conventional SGD optimizer, the starting learning rate is 0.001 and is divided by 10 after every 20 epochs. After 100 epochs, the training converges. The momentum is 0.9, and the batch size is 128. In all of the tests, we use a random horizontal flip strategy for data argumentation.

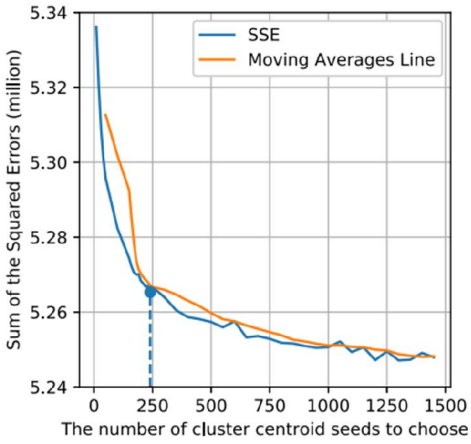

Fig. 6.1. The result of elbow method. The blue line shows that the SSE changes with the K, and the orange line is the MA line.

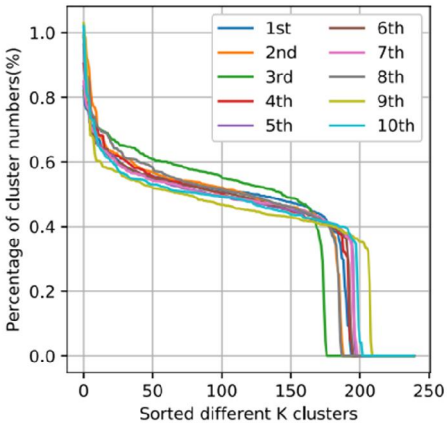

Fig.6.2. The percentage distribution results from ten experiments.

6.2 Experiment on PDD271.

1) In CRR, the choice of K: The Gaussian mixture model and K-means clustering are two well-known cluster methods. We picked K-means++ as the cluster algorithm in all of our trials due to the vast size of the dataset and the algorithm's stability. The value of K was calculated using the 'elbow' approach. The evident 'elbow' point in where K is 240 may be obtained from the sum of squared errors (SSE) and the trend line of SSE computed by the Moving Average (MA) method, as shown in Fig. 6.1.

IJARSCT
ISSN (Online) 2581-9429
International Journal of Advanced Research in Science, Communication and Technology (IJARSCT)
Volume 2, Issue 1, June 2022
Impact Factor: 6.252

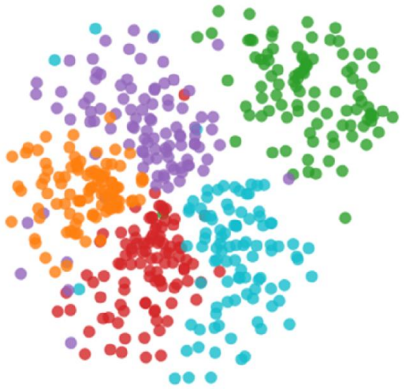

Fig.6.3. The t-SNE visualizations of the result of K-means clustering(randomly choosing five cluters).

TABLE II
PERFORMANCE COMPARISON FOR DIFFERENT TRAINING METHODS

Method	Validate(%)	Test(%)
ResNet152	88.63	83.37
w/o WSL	81.98	77.14
w/o Weights	89.07	84.96
TLR	**89.44**	**85.40**

We repeat the clustering operation ten times and find that the distributions of the clustering results are similar and stable, indicating that the clustering in this dataset has converged. In addition, Fig. 9 displays an t-SNE [40] clustering map using patch samples in five random clusters to qualitatively validate the clustering results.

2) TLR Evaluation: To assess TLR, we employed the following comparison.
• ResNet152 is a research network. This approach uses the entire image to finetune ResNet152.
• w/o WSL. Following the maxpooling and softmax layers, this technique employs the finetuned ResNet152 to directly extract the feature of each patch. 'Without Weakly Supervised Learning' stands for 'without Weakly Supervised Learning.'
• w/o Weights. This approach finetunes ResNet152 by using patches from all of the photos, and then extracts the feature of each patch using maxpooling and softmax layers. 'w/o Weights' refers to patch training without the use of weights.
Table II displays the experimental outcomes. We can see that (1) without WSL, performance suffers. The most likely rationale is that knowledge regarding backgrounds or healthy areas is negative for forecasting illness categories, and that blocking the information into patches exacerbates its influence.
(2) When compared to ResNet152, training on patches without weights enhances recognition performance. It demonstrates that for this task, weakly supervised learning is effective. (3) In both the validation and testing sets, TLR improves performance even more, demonstrating the benefit of loss reweighting in emphasising sick portions. (4) It is difficult to significantly enhance recognition performance due to the complexity, diversity, and variability of plant disease.

TABLE III
PERFORMANCE COMPARISON FOR INTEGRATION METHODS

Method	Validate(%)	Test(%)
LSTM	87.95	83.23
BiLSTM	89.70	85.50
sumBiLSTM	88.72	84.60
WFI	**89.91**	**85.54**

IJARSCT
ISSN (Online) 2581-9429
International Journal of Advanced Research in Science, Communication and Technology (IJARSCT)
Volume 2, Issue 1, June 2022
Impact Factor: 6.252

TABLE IV
ABLATION STUDY ON THE PDD271

Method	Validate(%)	Test(%)
w/o CRR	89.54	84.87
w/o TLR	89.23	84.98
w/o WFI	89.44	85.40
Full	**89.91**	**85.54**

3) WFI evaluation: We looked at how well LSTM and its variations, such as BiLSTM and sumBiLSTM, integrated patch feature sequences without reweighting.

WFI, on the other hand, takes the weighted patch feature sequence as its input. The suggested WFI gets the best recognition performance, as shown in Table III, and benefits greatly from the feature reweighting technique.

4) Ablation Study: We looked at the effects of ablation. CRR, TLR, and WFI are all components of our structure. The following are the different runs we created in the PDD271 datasets.

• w/o CRR. We use the trained baseline in this baseline. patch features from a network and then fusing them BiLSTM is a feature.

• w/o TLR. The reweighted baseline is replaced in this baseline. loss compared to the original loss during the unsupervised period in our framework for training

• w/o WFI. WFI is substituted by the in this baseline. In our framework, we have a layer called maxpooling.

5) State-of-the-Art Comparisons: We compare our method to state-of-the-art deep network topologies and fine-grained recognition models, as presented in Table V, for further verification of the proposed method. The findings reveal that (1) the SeNet154 outperforms other single networks because it can gather useful illness information using spatial-channel attention. (2) Without adding any attention modules, our strategy can boost the Resnet152's performance by 1.28 percent. We also switch the backbone network from Resnet152 to SeNet154, which is an attention model.

TABLE V
COMPARISON WITH THE RESULTS FOR STATE-OF-THE-ART DEEP NETWORK ARCHITECTURES AND FINE-GRAINED RECOGNITION MODELS ON PDD271

Method	Validate(%)	Test(%)
VGG16 [42]	85.51	79.80
ResNet50 [43]	87.96	82.75
ResNet152 [43]	88.63	83.37
WRN [44]	86.15	78.95
DenseNet161 [45]	89.79	85.43
GoogleNet [46]	86.74	81.56
PolyNet [47]	87.42	82.54
PNASNet [48]	89.41	84.44
SeNet154 [35]	89.95	84.63
WS-DAN(ResNet152) [33]	89.36	84.25
NTS-NET(ResNet152) [32]	84.10	81.30
DCL(ResNet152) [41]	89.86	85.00
Our Method(ResNet152)	89.91	85.54
Our Method(SeNet154)	**90.01**	**85.58**

TABLE VI
PERFORMANCE COMPARISON FOR DIFFERENT PATCH SIZES.4 × 4 MEANS THE IMAGE IS DIVIDED INTO 4 × 4 PATCHES, AND THE SIZE OF EACH PATCH IS 56 × 56 PIXELS

Method	Validate(%)	Test(%)
2 × 2	89.95	85.53
3 × 3	89.99	85.55
4 × 4	**90.01**	**85.58**

The results also demonstrate that integrating our technique with SeNet154 enhances testing performance by 1% (from 84.63 percent to 85.58 percent) and reaches state-of-the-art performance. This phenomena shows that our technique and attention-based methods can work together in a single framework to improve recognition performance even more. (3) In general, our method outperforms state-of-the-art fine-grained methods, such as the attention-based WS-DAN [33] and

IJARSCT
ISSN (Online) 2581-9429
International Journal of Advanced Research in Science, Communication and Technology (IJARSCT)
Volume 2, Issue 1, June 2022
Impact Factor: 6.252

the patch-based NTS-NET [32] and DCL [41]. This event demonstrates that our method is more suitable for plant disease recognition when the properties of the plant disease image are taken into account.

6) The Impact of Different Patch Sizes: Because patch size is a key component in avoiding missing diseases, we are examining the impact of different patch sizes.Each image is divided into two (2), three (3), four (4) patches, correspondingly. We do not check the smaller patch size due to computational complexity and receptive field. Table VI displays the outcome.

7) Patch Order Influence: In Table VII, we analyse the different patch feature sequence orders to see how they affect the patch feature sequence. We notice that the results for the various fixed orders are nearly identical. The order in which the patches are applied has no bearing on the final prediction.

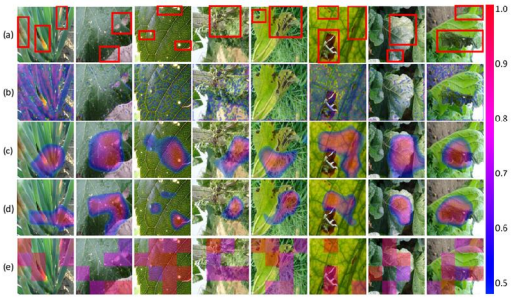

TABLE VII
IMPACT OF ORDERS. THE 'T', 'B', 'L', AND 'R' DENOTE THE TOP, BOTTOM, LEFT AND RIGHT, RESPECTIVELY. THE 'T2B,L2R' MEANS THE PATCHES FROM EACH IMAGE ARE ORDERED FROM TOP TO BOTTOM AND LEFT TO RIGHT. THE 'RD' DENOTES THE RANDOM ORDER. THE 'FIXED' DENOTES THAT THE ORDER OF THE PATCH LIST FOR EACH IMAGE IS FIXED, AND THE 'UNFIXED' DENOTES THAT THE ORDER OF THE PATCH LIST FOR EACH IMAGE IS UNFIXED

Method	Validate(%)	Test(%)
t2b,l2r,fixed	90.01	85.58
l2r,t2b,fixed	90.01	85.48
t2b,r2l,fixed	90.01	85.62
r2l,t2b,fixed	90.01	85.66
rd,fixed	90.02	85.62
rd,unfixed	**90.10**	**85.70**

The data's most startling feature is that the random unfixed order performs far better than the others. One probable explanation is that the plant is infected regardless of where the lesions emerge. Another rationale is that the unpredictability of the sequence is likely to boost the power of networks.

8) Visualization: We use a gradient-weighted class activation heatmap to depict distinct emphasised regions in different ways [49]. The visualisation results of various common deep architectures, such as VGG16 and ResNet152. The suggested cluster-based region reweighting strategy's reweighted maps, where we only visualise the patch x's weight when wx 0.75.

We discovered that the suggested reweighted maps can cover more discriminative regions than feature maps from standard deep networks. VGG16 and ResNet152 are likely to focus on disease-relevant regions while overlooking some essential information. Our method can pay attention to numerous dispersed regions, which is more ideal for detecting plant diseases. The PDD271 visualisation findings further prove the efficacy of the proposed cluster-based reweighting technique.

6.3 Use the PlantVillage Dataset to test your hypothesis.

In addition to the PDD271, we test our technique on another publicly accessible benchmark dataset, the PlantVillage dataset, to ensure that it is effective.

IJARSCT
ISSN (Online) 2581-9429
International Journal of Advanced Research in Science, Communication and Technology (IJARSCT)
Volume 2, Issue 1, June 2022
Impact Factor: 6.252

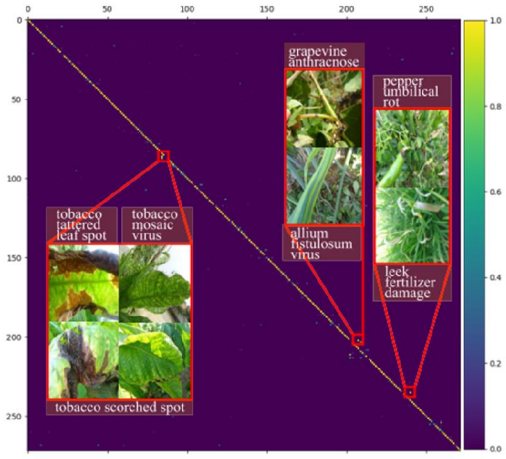

TABLE VIII
PERFORMANCE COMPARISON OF METHODS ON PLANTVILLAGE

Method	Test(%)
AlexNet [5]	99.24
DenseNet169 [45]	98.89
GoogleNet [46]	99.76
ResNet34 [43]	99.67
ResNet152 [43]	99.69
VGG13 [42]	99.49
Squeezenet [50]	99.20
Our Method(ResNet152)	**99.78**

There are 38 plant disease categories in the PlantVillage dataset, with a total of 54,309 photos. It is divided according to the setup in [12], with 80% of the dataset utilised for training and 20% for validation. Because all of the photographs are captured on the table, all of the approaches work well, as shown in Table VIII.

VII. CONCLUSION

Plant disease identification is a fascinating and useful topic. However, due to a lack of systematic inquiry and a large-scale dataset, this subject has not been properly investigated. The most difficult part of creating such a dataset is establishing a reasonable structure from both an agricultural and an image processing standpoint.

We investigate the topic of plant disease recognition in the community of image processing in this study. We created the first large-scale plant disease dataset with 271 plant disease categories and 220,592 photos with the support of agriculture specialists. We also provide a plant disease-oriented framework for recognising plant diseases based on their distinguishing traits. We devise an approach for computing patch weights based on the patch feature cluster distribution, and then use learnt weights to reweight both patch features and the loss to steer model optimization. The proposed method's efficiency is demonstrated by qualitative and quantitative evaluations on the PDD271 and PlantVillage datasets. In this project, we'll look at the many segmentation and classification strategies and algorithms that have been proposed to improve segmentation quality. However, the results show that, in comparison to the suggested graph cut model, segmentation approaches do not work well in large datasets and are difficult to implement. We have proposed a method for segmenting a leaf in a natural scene based on the optimization of a polygonal leaf model utilised as a shape prior for a precise of grab cut segmentation. It also provides a set of global geometric descriptors that, when combined with local curvature-based characteristics recovered from the final contour, can be used to categorise tree species.

REFERENCES

[1]. Z. Li et al., "Non-invasive plant disease diagnostics enabled by smartphone-based fingerprinting of leaf volatiles," Nature Plants, vol. 5, no. 8, pp. 856–866, Aug. 2019.

[2]. G. Litjens et al., "A survey on deep learning in medical image analysis," Med. Image Anal., vol. 42, pp. 60–

IJARSCT
ISSN (Online) 2581-9429
International Journal of Advanced Research in Science, Communication and Technology (IJARSCT)
Volume 2, Issue 1, June 2022
Impact Factor: 6.252

88, Dec. 2017.

[3]. W. Min, S. Jiang, L. Liu, Y. Rui, and R. Jain, "A survey on food computing," ACM Comput. Surv., vol. 52, no. 5, pp. 92:1–92:36, 2019.

[4]. E. Moen, D. Bannon, T. Kudo, W. Graf, M. Covert, and D. Van Valen, "Deep learning for cellular image analysis," Nature Methods, vol. 16, no. 12, pp. 1233–1246, 2019.

[5]. A. Krizhevsky, I. Sutskever, and G. E. Hinton, "ImageNet classification with deep convolutional neural networks," in Proc. Neural Inf. Process. Syst., 2012, pp. 1106–1114.

[6]. A. Bauer et al., "Combining computer vision and deep learning to enable ultra-scale aerial phenotyping and precision agriculture: A case study of lettuce production," Horticulture Res., vol. 6, no. 1, pp. 1–12, Dec. 2019.

[7]. S. Sladojevic, M. Arsenovic, A. Anderla, D. Culibrk, and D. Stefanovic, "Deep neural networks based recognition of plant diseases by leaf image classification," Comput. Intell. Neurosci., vol. 2016, pp. 1–11, May 2016.

[8]. J. Wang, L. Chen, J. Zhang, Y. Yuan, M. Li, and W. Zeng, "CNN transfer learning for automatic image-based classification of crop disease," in Image and Graphics Technologies and Applications. Beijing, China: Springer, 2018, pp. 319–329.

[9]. K. P. Ferentinos, "Deep learning models for plant disease detection and diagnosis," Comput. Electron. Agricult., vol. 145, pp. 311–318, Feb. 2018.

[10]. G. Wang, Y. Sun, and J. Wang, "Automatic image-based plant disease severity estimation using deep learning," Comput. Intell. Neurosci., vol. 2017, pp. 1–8, Jul. 2017.

[11]. M. RuBwurm and M. Korner, "Temporal vegetation modelling using long short-term memory networks for crop identification from mediumresolution multi-spectral satellite images," in Proc. IEEE Conf. Comput. Vis. Pattern Recognit. Workshops (CVPRW), Jul. 2017, pp. 11–19.

[12]. M. Brahimi, M. Arsenovic, S. Laraba, S. Sladojevic, K. Boukhalfa, and A. Moussaoui, "Deep learning for plant diseases: Detection and saliency map visualisation," in Human and Machine Learning. Cham, Switzerland: Springer, 2018, pp. 93–117.

[13]. W. Ge, X. Lin, and Y. Yu, "Weakly supervised complementary parts models for fine-grained image classification from the bottom up," in Proc. IEEE/CVF Conf. Comput. Vis. Pattern Recognit. (CVPR), Jun. 2019, pp. 3034–3043.

[14]. A. J. Wakeham, G. Keane, and R. Kennedy, "Field evaluation of a competitive lateral-flow assay for detection of alternaria brassicae in vegetable Brassica crops," Plant Disease, vol. 100, no. 9, pp. 1831–1839, Sep. 2016.

[15]. A. K. Lees, L. Sullivan, J. S. Lynott, and D. W. Cullen, "Development of a quantitative real-time PCR assay for phytophthora infestans and its applicability to leaf, tuber and soil samples," Plant Pathol., vol. 61, no. 5, pp. 867–876, Oct. 2012.

[16]. C. H. Bock, G. H. Poole, P. E. Parker, and T. R. Gottwald, "Plant disease severity estimated visually, by digital photography and image analysis, and by hyperspectral imaging," Crit. Rev. Plant Sci., vol. 29, no. 2, pp. 59–107, Mar. 2010.

[17]. F. Ahmad and A. Airuddin, "Leaf lesion detection method using artificial bee colony algorithm," in Advances in Computer Science and its Applications, vol. 279. Beijing, China: Springer, 2014, pp. 989–995.

[18]. S. Prasad, P. Kumar, and A. Jain, "Detection of disease using blockbased unsupervised natural plant leaf color image segmentation," in Swarm, Evolutionary, and Memetic Computing. Beijing, China: Springer, 2011, pp. 399–406.

[19]. A. Ramcharan, K. Baranowski, P. Mcclowsky, B. Ahmed, and D. P. Hughes, "Using transfer learning for image-based cassava disease detection," Frontiers Plant Sci., vol. 8, p. 1852, Oct. 2017.

[20]. E. Mwebaze, T. Gebru, A. Frome, S. Nsumba, and J. Tusubira, "iCassava 2019 fine-grained visual categorization challenge," 2019, arXiv:1908.02900. [Online]. Available: https://arxiv.org/abs/1908.02900.

[21]. D. P. Hughes and M. Salathé, "An open access repository of images on plant health to enable the development of mobile disease diagnostics through machine learning and crowdsourcing," 2015, arXiv:1511.08060. [Online].

[22]. H. Yu and C. Son, "Apple leaf disease identification through region-of-interest-aware deep convolutional

IJARSCT
ISSN (Online) 2581-9429
International Journal of Advanced Research in Science, Communication and Technology (IJARSCT)
Volume 2, Issue 1, June 2022
Impact Factor: 6.252

neural network," 2019, arXiv:1903.10356. [Online]. Available: https://arxiv.org/abs/1903.10356.

[23]. C. Xie et al., "Multi-level learning features for automatic classification of field crop pests," Comput. Electron. Agricult., vol. 152, pp. 233–241, Sep. 2018.

[24]. X. Wu, C. Zhan, Y.-K. Lai, M.-M. Cheng, and J. Yang, "IP102: A large-scale benchmark dataset for insect pest recognition," in Proc. IEEE/CVF Conf. Comput. Vis. Pattern Recognit. (CVPR), Jun. 2019, pp. 8787–8796.

[25]. J. Donahue et al., "Decaf: A deep convolutional activation feature for generic visual recognition," in Proc. Int. Conf. Mach. Learn., vol. 2014, pp. 647–655.

[26]. N. Zhang, J. Donahue, R. Girshick, and T. Darrell, "Part-based R-CNNs for fine-grained category detection," in Proc. Eur. Conf. Comput. Vis., 2014, pp. 834–849.

[27]. T. Xiao, Y. Xu, K. Yang, J. Zhang, Y. Peng, and Z. Zhang, "The application of two-level attention models in deep convolutional neural network for fine-grained image classification," in Proc. IEEE Conf. Comput. Vis. Pattern Recognit. (CVPR), Jun. 2015, pp. 842–850.

[28]. M. Lam, B. Mahasseni, and S. Todorovic, "Fine-grained recognition as HSnet search for informative image parts," in Proc. IEEE Conf. Comput. Vis. Pattern Recognit. (CVPR), Jul. 2017, pp. 6497–6506.

[29]. T.-Y. Lin, A. RoyChowdhury, and S. Maji, "Bilinear convolutional neural networks for fine-grained visual recognition," IEEE Trans. Pattern Anal. Mach. Intell., vol. 40, no. 6, pp. 1309–1322, Jun. 2018.

[30]. S. Jiang, W. Min, L. Liu, and Z. Luo, "Multi-scale multi-view deep feature aggregation for food recognition," IEEE Trans. Image Process., vol. 29, pp. 265–276, 2020.

[31]. W. Min, L. Liu, Z. Luo, and S. Jiang, "Ingredient-guided cascaded multiattention network for food recognition," in Proc. 27th ACM Int. Conf. Multimedia, Oct. 2019, pp. 99–107.

[32]. Z. Yang, T. Luo, D. Wang, Z. Hu, J. Gao, and L. Wang, "Learning to navigate for fine-grained classification," in Proc. Eur. Conf. Comput. Vis., Sep. 2018, pp. 438–454.

[33]. T. Hu and H. Qi, "See better before looking closer: Weakly supervised data augmentation network for fine-grained visual classification," CoRR, vol. abs/1901.09891, 2019.

[34]. Y. Peng, X. He, and J. Zhao, "Object-part attention model for finegrained image classification," IEEE Trans. Image Process., vol. 27, no. 3, pp. 1487–1500, Mar. 2018.

[35]. J. Hu, L. Shen, and G. Sun, "Squeeze-and-excitation networks," in Proc. IEEE/CVF Conf. Comput. Vis. Pattern Recognit., Jun. 2018, pp. 7132–7141.

[36]. G.-J. Qi, "Hierarchically gated deep networks for semantic segmentation," in Proc. IEEE Conf. Comput. Vis. Pattern Recognit. (CVPR), Jun. 2016, pp. 2267–2275